

# Recent Tendencies in the Use of the Response Surface Method in the Stability of a Synthetic Retaining Wall

M. Boutahir Born Bencheikh<sup>1</sup>, A. Aidoud<sup>2</sup>, S. Boukour<sup>3</sup>, N. Handel<sup>4</sup>, N. Khaldi<sup>5</sup>, M. Dorbani<sup>6</sup> and F.Z. Benarbia<sup>7</sup>

<sup>1</sup>University 8 May 1945, Laboratory of Civil Engineering and Hydraulics (LGCH), Guelma, Algeria

<sup>2</sup> University 8 May 1945, Laboratory of Civil Engineering and Hydraulics (LGCH), Guelma, Algeria

<sup>3</sup>Faculty of Science and Technology, Abdelhafid Boussouf Mila University Center, Algeria

<sup>4</sup>Department of Civil Engineering, INFRARES Laboratory, University of Mouhamed Cherif Messadia, Souk-Ahras, Algeria

<sup>5</sup>University 8 May 1945, Laboratory of Civil Engineering and Hydraulics (LGCH), Guelma, Algeria

<sup>6</sup>University 8 May 1945, Laboratory of Civil Engineering and Hydraulics (LGCH), Guelma, Algeria

E-mail: Bencheikh2005@yahoo.fr

**ABSTRACT:** Geogrids, a type of geosynthetic material composed of polymers, have found extensive use in transportation, infrastructure, and structural projects. They are commonly employed for soil stabilization purposes, ranging from reinforcing walls to strengthening subgrade soils or embankments. There is also a growing potential for geogrids to be utilized in remote sensing applications. To predict the horizontal displacement ( $U_x$ ) and safety factor ( $F_s$ ) of a synthetic retaining wall, finite element software is utilized for studying the impact of soil properties and reinforcement parameters, the vertical spacing between reinforcements ( $S_v$ ), their length ( $L$ ), and their normal stiffness ( $E_A$ ). The extent of influence from various factors is assessed through a grey relational grade analysis. Subsequently, the input layer parameters for the response surface methodology (RSM) of the central composite design (CCD) type are determined based on the outcomes of the grey relational grade analysis. The horizontal displacement and safety factor are predicted using numerical simulation with Plaxis 2D results. This paper presents a study of a synthetic retaining wall using an composite central type fractional digital experiment plan. The functional relationship between the output variables (horizontal displacement and safety factor) and the input variables ( $L$ ,  $S_v$ ,  $E_A$ ) was expressed with determination coefficients ( $R^2 = 99.63\%$  for  $U_x$  and  $R^2 = 99.95\%$  for  $F_s$ ). These coefficients represent the ratio between the variation due to the model and the total variation. This high level of determination indicates that the model is well-fitted for both responses, confirming its adequacy. Therefore, central composite design models can be adopted to solve geotechnical problems, especially those related to synthetic retaining walls, which possess a highly complex and nonlinear structure.

**KEYWORDS:** Variance analysis, Identification of parameters, Optimization, Synthetic Support, and Reinforcement.

## 1. INTRODUCTION

Until the end of the 9th century, soil retention was achieved solely through the weight of a massive structure. Following the invention of reinforced concrete and its rapid development in the early 20th century, reinforced concrete retaining walls were constructed, in which soil above the backfill contributes to the wall's stability. However, the entire lateral pressure is absorbed by the reinforced concrete panel. In 1963, Henri Vidal (Leshchinsky, 2004) combined sturdy metal reinforcements capable of withstanding tension, giving birth to a new composite material: reinforced soil.

The first application of a geotextile, a thick cotton weave, in road construction was in 1926 (Beckham, 1935) by the Department of Highway Research in South Carolina. Until the deterioration of the weave, the road remained in good condition and the use of the geotextile has significantly reduced localized cracks and breaks in the pavement. A geotextile made from synthetic fibers with functions in filtration and protection against coastal erosion was used in 1950 in Florida (Barret, 1966). This application against erosion was then widely developed in the 1960s. In Europe, the first applications of geotextile materials were made in the early 1960s in the construction and renovation of large embankments and dykes for the protection of lowlands along the North Sea coast of the Netherlands, after the major floods in the winter of 1953 (Gicot, 1982). So the geosynthetics have been used in a wide range of applications such as transportation, geotechnical, environmental and hydraulics (Jongvivatsakul *et al.*, 2018). Many geosynthetic materials have been developed to stabilise soil slopes while also being environmentally friendly and convenient for construction (Ngo, 2019).

Recently, Ramdit (Jirawattanasomkul *et al.*, 2019) and Jongvivatsakul *et al.* (Jirawattanasomkul *et al.*, 2019) have introduced a manufactured made GCCM, which comprised of two geotextile layers and cement powder. The top non-woven geotextile, the middle cement powder layer and the bottom woven geotextile

are fabricated by hot needles punching. In the final product, the GCCM in a sandwich manner has a uniform thickness and a relatively light weight. The GCCM must be hydrated by water spraying after installing on ground to make it harden (Jirawattanasomkul *et al.*, 2019). Due to its high stiffness, strength and water tightness, the GCCM has been employed in many geotechnical application such as slope protection and soil erosion control (Jirawattanasomkul *et al.*, 2019). Since the GCCM is a manufactured product, its properties is more uniform comparing with other in-placed slope protection materials like shotcrete. In addition, the GCCM has relatively light weight, so it is simple to install in the slope area. However, the numerical study of GCCM is still limited, and the constitutive model and its parameters are important for FEA (Jirawattanasomkul *et al.*, 2019).

Another technique developed in the field of geotechnics which is geosynthetic-reinforced granular fill-soft soil system is now being used frequently and in recent years, geosynthetics have seen rapidly increasing usage in geotechnical engineering applications (Ngo *et al.*, 2023) as base for unpaved roads, shallow foundation, storage tanks, heavy industrial equipment, in embankment fills and car parks. The purpose of the fill is to provide a suitable operating surface on which concentrated loads may be carried without the subgrade failing or deforming excessively (Laxmikant, 2013). It is now common practice to use layer of geotextile or geogrid at the base or within the fill layer to improve its bearing capacity by the structural action of geogrid. The behaviour of such a system is complex and number of study have been done notably by (Giroud, 1981); (Fragaszyand, 1984); (Love, 1987); (Verma, 1986); (Carroll, 1987); (Mahmoud, 1989); (Mandal, 1995), and other researchers such as (Sukkarak, 2021) study the feasibility of a geogrid-encased deep cement mixing (EDCM) pile for enhancing the load-carrying capacity (Qult) of a conventional deep cement mixing (DCM) pile, the geogrid encasement effectively improves the Qult of the DCM piles by a factor of two. With the additional confinement provided by the

geogrid encasement, the geogrid can also provide a greater contribution to the loading transfer. The increase in  $Q_{ult}$  became more significant with a lower strength of the DCM (Sukkarak, 2021). The same thing a research developed by (Jirawattanasomkul *et al.*, 2018) used a model by a finite element modelling of a new geosynthetic cementitious composite material called GCCM. The framework adopted a concept of concrete externally bonded by fibre-reinforced polymer (FRP). The existing bond-slip model was used to predict a flexural behaviour of GCCM. The geosynthetic reinforced soil retaining walls are greatly appreciated thanks to their effective performance, high resistance to dynamic loading and economic benefit compared to the conventional retaining walls (Masini, 2015; Santhanakumar, 2015; Gaudio, 2018). They are used for transportation construction like in roads, highways, bridges and railway structures, as well as for industrial and protective structures, for dams, mining structures, in addition to their use for commercial and public structures. The vital role of geosynthetic reinforced soil walls, can be explained by their multiple applications. Safety constitutes the great challenge of the urban development space (Hicham Alhajj, 2016).

Reinforced soil retaining walls are structures composed of structural (retaining walls) and geotechnical (soil reinforcement) elements. This construction technique has become popular since its invention by the French architect and engineer Henri Vidal in the early 1960 (Leshchinsky, 2004). The construction method is based on the association of a compacted backfill and strip reinforcement elements connected to the wall facing. The reinforcements improve significantly the soil mass shear strength due to the soil reinforcement interaction. The reinforcements generally used in these structures are made of steel (inextensible materials). However, in aggressive environments, these metal reinforcements are replaced by non-corrodible geosynthetic reinforcements, which have a higher extensibility than the metal ones (Hicham Alhajj, 2016).

The primary objective of the preceding studies is to investigate the impact of certain parameters on the stability of a synthetic retaining wall. The obtained results demonstrate that greater stiffness in the facing corresponds to increased wall stability. The forces within the reinforcement elements amplify with the increased stiffness of the facing, particularly at the connection points situated behind the facing. Furthermore, the line of maximum traction approaches the facing as its stiffness becomes greater.

Numerous studies involving both reduced and full-scale models, subjected to head overloading or not, have examined the effects of reinforcement density and load inclination (Huang, 2004). These studies have revealed that structural stability increases with higher reinforcement density. In cases of models subjected to head overloading, reducing the vertical spacing between reinforcement layers enhances critical height and load-bearing capacity.

(Abe, 2017a), after a series of tests on walls reinforced by centrifugal geosynthetics overloaded uniformly on the surface, studied the influence of the length of reinforcement on the stability, he concludes that the stability of such structures requires a minimum aquifer length, and beyond a certain aquifer length, the contribution is negligible. (Abe, 2017B) also concludes that the failure surface, for all of these tests, is flat and that the angle of inclination, measured relative to the vertical, is a function of the lengths of the reinforcement plies. We also note that with respect to the horizontal the fracture surfaces make angles between 51.5 and 62 degrees.

(Wilson-Jones, 1992), carried out a series of tests on two-dimensional analog scale models of Schneebeli without overhead overload by varying the inclination of the facing ( $\beta = 60^\circ, 80^\circ$  and  $90^\circ$ ) and the length of the layers. Scale models reinforced by metal reinforcements have also shown that the length of the reinforcements does not bring any gain in stability beyond a certain limit.

The influence of reinforcement stiffness has been analyzed by several authors (Bingquan, 2009; Bathurst, 2009, Hardiyatmo, 1995). The rigidity of the reinforcement improves the stability of the structures. To better understand the mechanisms of reinforcement by flexible inclusions, (Bingquan, 2009), carried out two tests on scale

models of walls with vertical facing and enveloped face, overloaded locally at the top. Two geotextiles with different mechanical characteristics were used ( $T_f = 2.8$  kN/m,  $\epsilon_f = 25\%$  and  $T_f = 5.1$  kN/m,  $\epsilon_f = 40\%$ ). The breaking load of the model reinforced by the geotextile ( $T_f = 5.1$  kN/m) is significantly higher. The dismantling of the two models, after rupture did not reveal any rupture of the water table, the ruin of the two models occurred by lack of anchoring.

With the increasing growth in the use of science and technology in solving everyday life problems, the need for methods that understand complex and ambiguous problems becomes greatly inevitable. Soft computing is an emerging collection of various methodologies aimed at finding a balance to poor precision, uncertainty, and unclear truth by applying a collection of statistical, probabilistic, and optimization tools in analyzing sets of data, classify the data, identify new patterns and predict next trends within the shortest convenient time.

Optimization leads to the maximizing or minimizing of functions by choosing input values or functions from a certain parameter set or range. Different deterministic and stochastic optimization schemes are available (Boumezerane, 2022), (Lakhal, 2017). Popular deterministic approaches are response surface methods, gradient-based strategies and others. On the other hand, typical stochastic approaches are widespread and they include: evolutionary algorithms, neural network approaches, particle swarm algorithms or the fuzzy logic theory-based methods. Optimization can be mono-objective where an optimum is searched for one function or multi-objective, where an optimum is searched not only for one parameter or function, but for several and sometimes also contradictory objective functions (Pareto optimization) (Boumezerane, 2022).

(Wong, 1985) performed reliability analysis of soil slopes using response surfaces method (RSM). (Humphreys, 1993) analysed a slope stability problem using results of finite difference method and regression analysis (Lakhal, 2011), (Tandjiria, 2000) used response surface method for reliability analysis of laterally loaded piles. (Sivakumar, 2007) presented a study on the analysis of allowable bearing pressures on shallow foundation using response surface method.

Response surface methodology (RSM) is an optimization procedure, which represents empirical modeling, that can be used to develop a relationship between process factors and experimental output (Abdulhameed, 2021). RSM has been one of the most useful tools to explain and establish the mathematical relation between input variables and the output responses (Adamu *et al.*, 2021). One of the advantages of RSM is that it is more beneficial in the conditions where there is need to investigate the effect of several variables on one or more responses to minimize the number of experiments required (Adamu *et al.*, 2021). The individual and combined effect of independent variables on desired response parameters were measured to build a mathematical model (Ebba, 2022). RSM has many advantages over the traditional time-consuming approach of analyzing one variable at a time: cost-effective and time-saving approach with less number of experimental runs, assessing the interaction effect of the independent variables on desired response, and modeling of the selected responses (Ebba, 2022), (Ghelich, 2019). The central composite design (CCD) and Box-Behnken design (BBD) are the most common design types of RSM (Ebba, 2022), (Somayajula, 2012). The CCD method is made of a two-level factor design and each factor has five different levels. CCD usually have axial points outside the "cube", which tests at extreme conditions and those points may not be in the region of interest. On the other hand, in the BBD method, each factor has three different levels and no axial points outside the specified limits. The BBD method is more practical because it often requires fewer design points to fall within the operating range and the number of experiments in the BBD method is usually less than that in CCD (Salari, 2022).

The object of this work concerns the numerical modeling and the optimization of the parameters influencing the stability of a

retaining wall reinforced by geogrid, by the use of the method of the response surfaces via the numerical plans of experiments. Initially through the determination of a geotechnical model, said reference and to develop a numerical model to simulate the behavior of the reinforced wall, and secondly the choice of a plan of numerical experiments as a support for modeling the wall based on the reinforcement parameters, namely the vertical spacing between reinforcements (S<sub>v</sub>), its length (L) and its normal stiffness (EA). The use of experimental plans leads to establishing a plan, including the maximum precision in the results with a minimum of experiments.

For our study, according to our parameters, a composite central-type response surface plan L26, contains an incorporated factorial or fractional plane with central points increased by a group of star points allowing the curvature to be estimated. The statistical tool analysis of variance (ANOVA) was used to analyze the obtained results.

## 2. METHODS AND MATERIALS

### 2.1 Modeling by Plaxis 2D

The use of numerical methods, the elasto-plastic finite element analysis and the limit analysis finite element method are the most comprehensive approach to investigate the performance of reinforced soil walls under seismic loading. The use of the numerical limit analysis remains limited in engineering practice. Many studies are conducted in the literature to assess numerically the performance of reinforced soil retaining walls under static and dynamic loading (Hicham Alhajj, 2016).

Several studies of the failure behavior of cell walls reinforced with geosynthetics are digitally processed using software including: code Finite element (FEM, Plaxis) (Guler, 2002). The fracture mechanisms obtained are compared with classical design methods at limit equilibrium. In the case of cohesive or pulverulent backfill materials, the failure mechanisms developed numerically tend towards a sliding mechanism.

The same approach is presented by on a structure (Guler, 2002) with cellular facing with connections to the reinforcements by HDPE geogrids. Analysis using a finite element code (SAGE) makes it possible to locate the most stressed level of reinforcement and to obtain critical values 20% lower than those given by the classic dimensioning method (CARTAGE).

### 2.2 Design Experiment (Central Composite Design – CCD)

In statistics, a central composite design is an experimental design, useful in response surface methodology, for building models, evaluating the effects (Lakehal, 2017) of factors and searching for the optimum conditions for the response variable without needing to use a complete three-level factorial experiment; this technique has been successfully used in slope stability analysis. A prior knowledge and understanding of the process and the process variables under investigation are necessary for achieving a more realistic model. In this study, CCD is performed to estimate the performance function of the quadratic model for optimizing the process. The independent variables are transformed into code level range from -1 to +1 interval where the low and high levels code as -1 and +1, respectively (Lakehal, 2017). The axial points are located at the value of + $\alpha$  and - $\alpha$  where  $\alpha$  is the distance of the axial point from the centre and performs the design rotatable in this study we use the characteristic of face centered star point, the centre points coded as 0. In this study a 2(m) + 2\*(m), two levels; (m) variable were used, for two variables, the model obtained was expressed as follows (Lakehal, 2017):

$$Y = a_0 + a_1 X_1 + a_2 X_2 + a_{11} X_{11}^2 + a_{22} X_{22}^2 + a_{12} X_{12}^2 \quad (1)$$

Where (Lakehal, 2017): Y = the measured response,  $a_0$  = the intercept term,  $a_1, a_2$  = linear coefficients,  $a_{12}$  = the logarithmic coefficient,  $a_{11}, a_{22}$  = quadratic coefficients,  $X_1, X_2$  = coded independent variables.

### 2.3 Stability of a Synthetic Retaining Wall and Design Experiment

Plaxis 2D modeling method linking with design experiment (central composite design), was applied to estimate the effect of main geotechnical parameters on safety factor with a geometric designs of (the calculation model) Figure 1 shows the profile type used in the simulation process by Plaxis 2D software .

In this study, a set of input and output data are prepared, and a central composite design CCD is used for developing the function of the quadratic model, the effect of variation of materials properties are studied (Lakehal, 2011). All data selected for developing the function of the quadratic model are obtained from stability analyses of 26 cases of stability of a synthetic retaining wall using the commercial software Plaxis 2D. the geotechnical properties of construction materials are given in Tables below.

## 3. CHARACTERISTICS OF MATERIALS

The characteristics of material predicted for numerical modelling included the structural elements material, soil and interface parameters and geogrid elements. The parameters used in the wall are briefly described in the following section.

### 3.1 Parameters of Structural Elements (the Wall)

We are going to model the wall by plate element with a linear elastic (Table 1) behavior model. This model is characterized by two properties, A normal stiffness EA and a bending stiffness EI.

**Table 1 Characteristics of the wall**

Parameters	Name	Unit	Value
Type of behavior	Material Type	-	Elastic
Normal stiffness	EA	KN/m	$6,6 \times 10^5$
bending stiffness	EI	KNm <sup>2</sup> /m	$4,95 \times 10^3$
Poisson ratio	v	-	0,15
Dry unit weight	$\gamma$	kN/m <sup>3</sup>	24
Weight	W	KN/m/m	7,2
Thickness	D	M	0.3

### 3.2 Reinforcement Geogrids

Geogrids are modeled using structural elements called “geogrid” in plaxis software (Table 2). These elements have only one necessary property, it is the axial stiffness EA.

**Table 2 Characteristics of geogrids**

Parameters	Name	Value	Unit
Type of behavior	Material Type	-	Elastic
Normal stiffness	EA	1000	kN/m

### 3.3 Soil and Interface Parameters

The behavior of the soil is characterized by the parameters summarized in Table 3. A perfectly plastic elastic linear model with the Mohr-Coulomb plasticity criterion included in the PLAXIS code is used to model the behavior of the different soil layers.

**Table 3 Soil parameters**

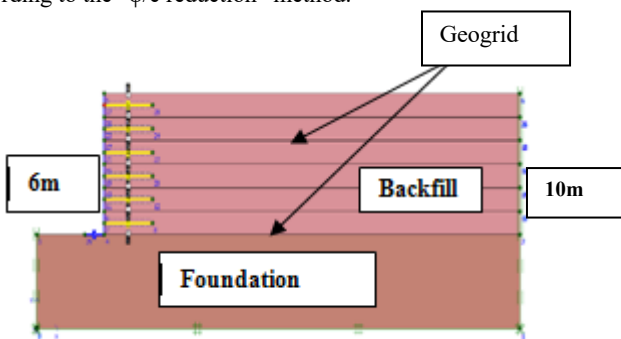
Parameters	Name	Unit	Backfill ( Sand)	Foundati on soil
Model type	Model	-	Mohr- Coulomb	Mohr- Coulomb
Type of behaviour	Type	-	Drained	Drained
Dry unit weight	$\gamma_{\text{unsat}}$	KN/m <sup>3</sup>	17	18
Saturated unit weight	$\gamma_{\text{sat}}$	KN/m <sup>3</sup>	20	21
Young's modulus	Eref	KN/m <sup>2</sup>	$3 \times 10^4$	$6 \times 10^4$
Poisson ratio	v	/	0.30	0.30
Cohesion	C	KN/m <sup>2</sup>	1	25
Friction angle	$\varphi$	(°)	35	20
Angle of dilatancy	$\Psi$	(°)	0	0

#### 4. GEOMETRY OF THE MODELED WALL

Figure 1 illustrates the cross section of the studied models geometry. A 15 noded triangular element is selected in this analysis. The global coarseness is set to medium, thus the number of elements generated (Surarak *et al.*, 2012) is approximately 2345 elements. It should be noted that the analysis will be carried out in "plain strains" or axisymmetry; the figure shows the boundary conditions. The vertical limit of the model is fixed in the horizontal direction but free to move in the vertical direction, at the base the model is assumed to be fixed in both directions (horizontal and vertical).

The case studied consists in analyzing the behavior of a retaining wall reinforced by geogrids. The model is made up of two layers, an embankment with a height of H=6 m reinforced by a standard wall with an L-shaped vertical facing and 6 layers of geogrids, the foundation soil with a height of h=4 m and 30 m in length presented in Figure 1. The reinforcement of this wall was carried out by layers of geogrids spaced 1m vertically and extending over a length of: L= 0.5×6 = 3m. Concerning the boundary conditions, the displacements at the base of the model are blocked in both horizontal and vertical directions, while only horizontal movements are blocked on the side edges.

The digital model is continuously updated by adding the ground and the geogrid sheets in stages, which represents the order of construction of the actual walls. The first reinforcement layer is always installed at an altitude of 0.50 m on the first layer of soil and the first block of the wall. Then, layers of geogrid are installed according to the spacing of reinforcement  $S_v = 1\text{m}$  up to the total height of the backfill. The last phase includes a safety analysis according to the " $\phi/c$  reduction" method.

**Figure 1** Numerical model components

#### 4.1 Numeric Program

In this study, according to our parameters, we chose a response surface plan of the central composite L26 type. For this purpose, it is first necessary to choose the factors and their levels of variation, our model comprises three factors of influence (the length of the geogrids (L), the spacing between the geogrids (Sv) and the normal

rigidity of the geogrids (EA) and each factor has two levels (max and min), the variation interval of each parameter of which is presented in the Table 4.

**Table 4 Range of variation of the parameters to be optimized**

Input Parameters	Levels of variation	
	Minimum value	Maximum value
L (m)	3	9
Sv (m)	1	2
EA(KN/m)	2000	4000

#### 5. RESULTS AND DISCUSSIONS

In this study, a composite central type response surface (L26) panel was chosen. of three parameters, with two modalities by parameters and the number of interactions make it possible to find the plan best adapted to the problem of the wall reinforced by geogrids. Each line corresponds to a model to be produced digitally by the Plaxis 2D software, so 26 digital models must be produced in accordance with the data in the Table 5. The results of the modeling in terms of horizontal displacement and the safety factor are presented in Table 5. These results are obtained following the various combinations in accordance with the matrix of planning of the experiments for a plan of response surface type central composite L26.

**Table 5 Plan of experiments L26 in parameter values**

N°	Factors		Responses		
	L (m)	Sv(m)	EA(KN/m)	Ux (m)	Fs
1	9	1	2000	0,6892	2,48
2	9	1	3000	0,9050	2,47
3	9	1	4000	0,8210	2,47
4	9	1,5	2000	1,0150	2,47
5	9	1,5	3000	1,2500	2,48
6	9	1,5	4000	0,9908	2,47
7	9	2	2000	0,4790	2,43
8	9	2	3000	0,6230	2,45
9	9	2	4000	1,1000	2,45
10	6	1	2000	1,7631	2,14
11	6	1	3000	1,1252	2,14
12	6	1	4000	1,7170	2,14
13	6	1,5	2000	1,8010	2,13
14	6	1,5	3000	1,1100	2,13
15	6	1,5	4000	1,1700	2,13
16	6	2	2000	0,7800	2,10
17	6	2	3000	2,0700	2,10
18	6	2	4000	1,2370	2,09
19	3	1	2000	0,1870	1,69
20	3	1	3000	0,9850	1,68
21	3	1	4000	1,9500	1,69
22	3	1,5	3000	0,3620	1,63
23	3	1,5	4000	1,5500	1,63
24	3	2	2000	0,2240	1,58
25	3	2	3000	0,2370	1,58
26	3	2	4000	0,5640	1,59

#### 5.1 Influence of Geogrid Length

In order to understand the effect of geogrid length on wall response, models with different lengths were analyzed with vertical spacing  $S_v=1\text{m}$  and  $L/H$  ratios of 0, 67, 1 and 1, 5, respectively.

The reading of the calculation results for the two cases of the spacing ( $S_v=1\text{m}$  and  $S_v=0,5$ ) is presented in Figure 2 below.

It can be seen from the graph that when the layers of the geogrids have a spacing of 1m, the wall undergoes a greater displacement compared to the wall for which the geogrids have a spacing of 0,5 m. Whereas in the first case ( $S_v=1\text{m}$ ) we note that when the length of the sheets decreases, there is an increase in the displacement of the wall, which is more significant when  $L$  goes from 6m to 9m.

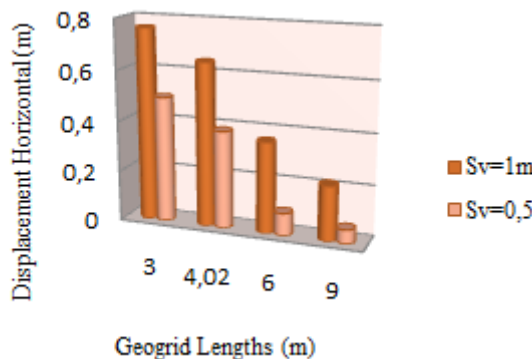


Figure 2 Horizontal displacement of the wall for different length cases

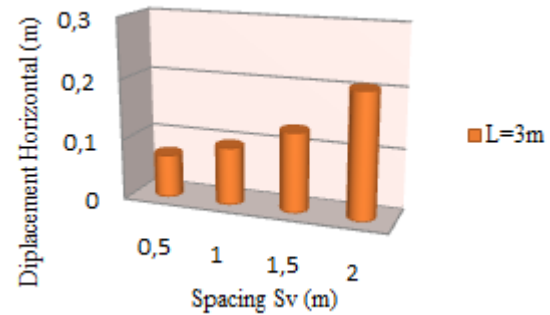


Figure 4 Horizontal displacement of the wall for different spacing cases

The vertical spacing between the horizontal layers of geogrids has a non-negligible and very remarkable effect on the behavior of the reinforced wall and on its overall stability. Decreasing the vertical spacing means increasing the number of geogrid layers. The number of layers for a spacing of 1 m is twice that of 2 m. It is obvious that this increase in the number of layers contributes to the stabilization of the wall and to the reduction of the horizontal displacement of the wall (See Figure 4). The results obtained show that the horizontal displacement is inversely proportional to the spacing between the layers.

In the other hand (Figure 5), it can be concluded that the calculated values of the safety factor decrease when the spacing increases, It's results are similar to those of (Surarak *et al.*, 2012).

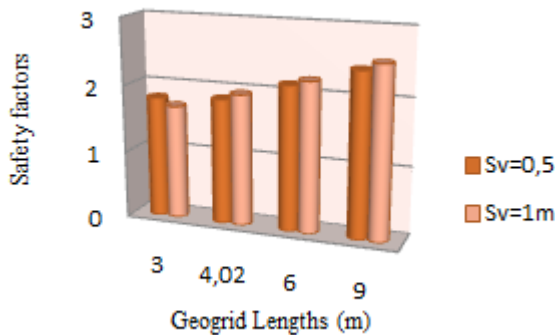


Figure 3 Safety factors depending on the length (  $S_v=1\text{m}$  and  $S_v=0,5\text{m}$  )

It should be noted that through the manipulation of geogrid layer lengths, we observed corresponding variations in safety coefficients (Figure 2). Calculated safety coefficient values increase as the length of the geogrids increases. Your original paragraph is already quite clear, but this rephrasing might help avoid any potential confusion.

## 5.2 Influence of Vertical Spacing between Geogrid Sheets

In this phase of the study, the length of the geosynthetic layers is constant ( $L=3\text{ m}$ ) according to the dimensioning method:  $L=0.5*H=0,5 \times 6 = 3\text{ m}$ .

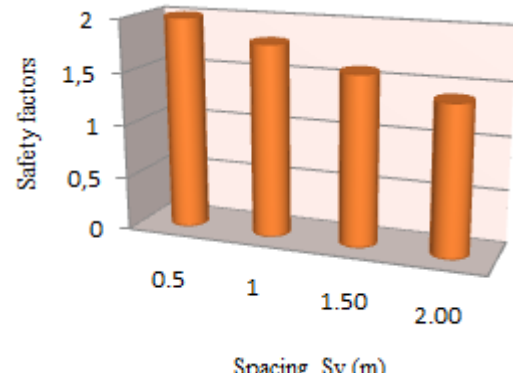


Figure 5 Safety factor as a function of spacing  $S_v$  ( $L=3\text{m}$ )

In what follows, the spacing between geogrids is varied, and for each spacing by varying the length, the choice of the spacing between the layers of reinforcements is made for four values ( $S_v=0,5$ ,  $S_v=1,50\text{m}$  and  $S_v=2,00\text{m}$ ) and an  $L/H$  ratio having the values 0,5, 0,67, 1 and 1,5. The results obtained represented in the form of a graph in Figure 6 for different models.

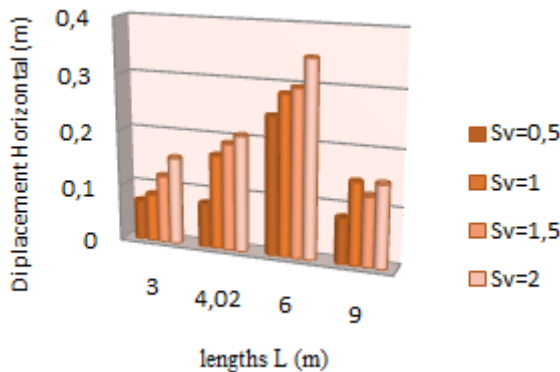


Figure 6 Horizontal displacements of the wall for different cases of lengths

The use of a number of reinforcement sheets in the ground seems to have a slight influence on the evolution of the horizontal displacement in the structure, especially at the level of the location of the geogrids. Indeed, increasing the number of layers of geogrids reduces this displacement and therefore acts in the direction of the stability of the structure (the spacing of 0.5m is the spacing which gives the minimum displacements).

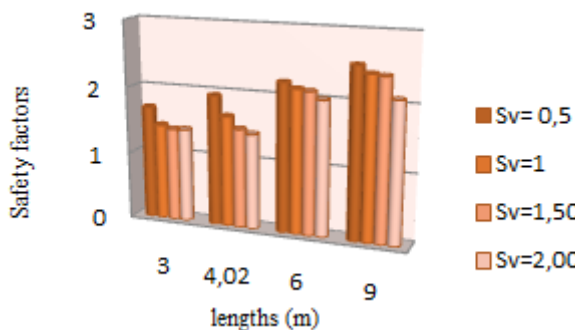


Figure 7 Safety factor according to spacing

According to the graphs of Figure 7 we can deduce that the safety factor increases when the length of geogrid increases and when we increase the length of the layers of geogrid and we decrease the spacings we see that the safety factor increases it's results are similar to those of (Hicham Alhajj, 2016).

### 5.3 Influence of Normal Geogrid Stiffness Normal Geogrid Stiffness

In this phase we change the normal stiffness of the geogrid to see their influence on the reinforced wall ( $L=3m$  and  $Sv=1m$  are fixed from the previous study), the normal stiffness of the geogrid varies as follows:  $EA=(2000\text{KN/m}, 3000\text{KN/m} \text{ and } 4000\text{KN/m})$ .

The influence of the stiffness on the horizontal displacement in the stabilized and reinforced soil mass is given in Figure 8, The results of the simulations show that the horizontal displacement of the wall decreased when the stiffness of the geogrids increases and clearly shows the importance of geogrid stiffness it's results are similar to those of (Hicham Alhajj, 2016).

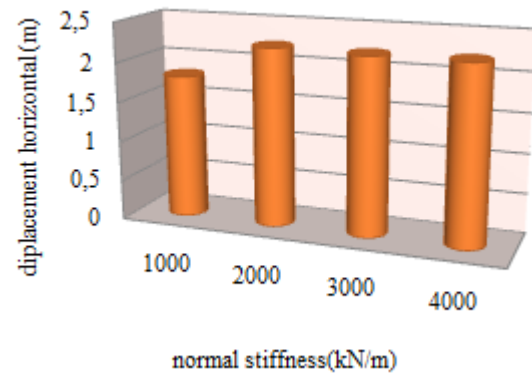


Figure 8 Safety factor according to normal stiffness ( $L=3\text{m}$ )

It should be noted that by varying the normal stiffness of the geogrids we recorded a variation in the safety factors (Figure 9). The calculated values of the safety factor indicate that by increasing the axial stiffness (EA) and keeping the constant spacing between geogrids, it is found that the safety factor increases until the axial stiffness reaches 2000 KN/m where it becomes constant and which gives better stability.

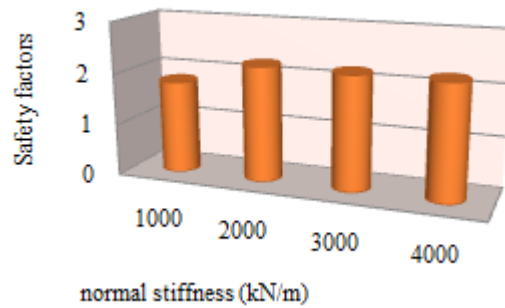


Figure 9 Safety factor according to the Normal stiffness of geogrids ( $L=3\text{m}$ )

We note that in the case of high rigidity geogrids ( $EA=4000\text{ kN/m}$ ) spaced 0.5m and 1m apart, the displacement of the wall is low with a slight increase whatever the length of the geogrid (6 m or 9 m).

However, in the case of low stiffness, the displacements are inversely proportional to the length and the spacing between them.

### 5.4 Influence of the Mechanical Properties of the Reinforced Soil Mechanical Properties of the Reinforced Soil (Backfill)

The influence of the mechanical properties of the reinforced embankment, is analyzed in this study, we keep the same parameters as the previous one except the change of the mechanical properties of the soil (the embankment, case of a coherent soil), and the same data which already fixed from the previous study ( $EA= 1000\text{KN/m}$ ,  $Sv=1\text{m}$  and  $L=3\text{m}$ ).

The length of the geogrid sheets is:  $L/H=0,5$  ( $L=3\text{m}$ ) ;  $L/H=0,67$  ( $L=4,02$ ) ;  $L/H=1$  ( $L=6\text{m}$ ) and  $L/H=1,5$  ( $L=9\text{m}$ ), the axial stiffness of, the geogrid  $EA = 1000\text{ kN/m}$ , the cohesion  $C = 35\text{ kN/m}^2$ . And the angle of friction  $\phi=5^\circ$ .

Examples of the distribution of horizontal displacements and the safety factors in this case for different lengths of the geogrids, and spacing  $Sv$  are shown in the Figure 10 below.

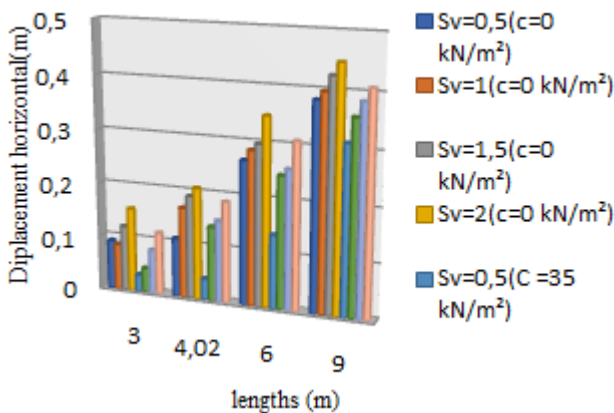


Figure 10 Comparison of horizontal displacements

We note that in the case of cohesive soils ( $C=35\text{kN/m}^2$ ), the horizontal displacements of the wall decrease almost by about 12% mm compared to pulverulent soils which reach higher values when the spacing is large (spacing of 2m) regardless of the variation in length (see Figure 10). We can deduce that for a coherent soil the horizontal displacement see very significant decreases depending on the spacing of the layers of geogrids as well as their length.

In the case of cohesive soils, the variation of safety factors has practically the same trend, it should be noted that when the granular backfill varies with a coherent backfill, the safety factor increases, thus promoting safety (Figure 11). Its results are similar to those of(Hicham Alhajj, 2016).

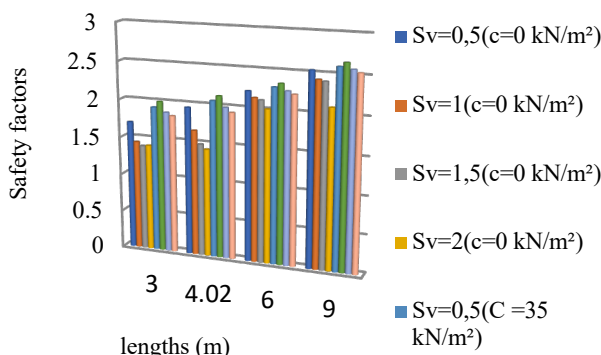


Figure 11 Comparison of safety factors

## 5.5 Influence of Overload

A uniformly distributed overload (Bencheikh, 2021) of 50 kPa is applied to the surface of the soil mass over a width  $B=6\text{m}$ . The data already fixed from the previous study ( $EA=1000\text{KN/m}$ ).

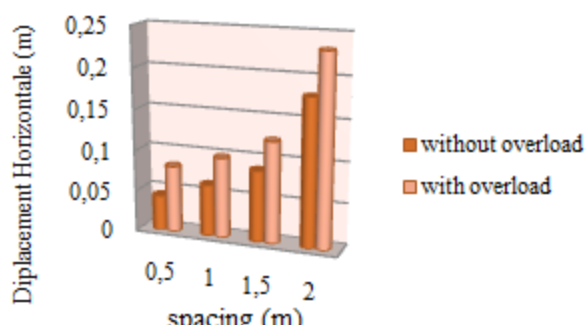


Figure 12 Horizontal displacement behind the wall without and with overload for  $L=3\text{m}$

In Figure 12, it can be clearly seen that the horizontal displacement of the wall increases with the presence of the live load.

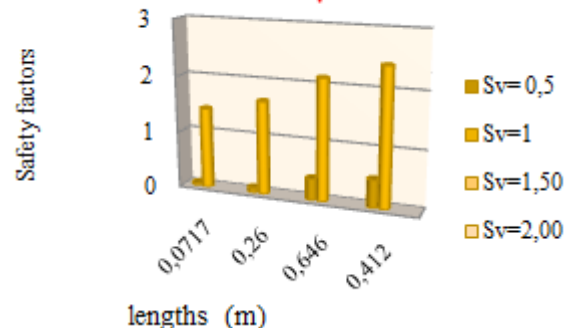


Figure 13 Safety factor according to the lengths without and with overload

From the graphs in Figure 13, it can be deduced that the safety factor with overload decreases compared to the safety factor without overload, this is logical because the presence of the overload has a considerable influence on the stability of the wall.

## 6. STATISTICAL ANALYSIS AND RSM MODELING ANOVA RESULTS

The accuracy of the model was further justified through analysis of variance (ANOVA). For the two response surfaces models of safety factor and horizontal displacement  $U_x$ , The analysis of variance ANOVA presented in Tables 6 and 7, The statistical significance of quadratic prediction models is evaluated using the P-value and F-value from ANOVA (Ebba, 2022).In the ANOVA table, the P-value represents the probability (ranging from 0 to 1) that the observed results in a study (or more extreme results) could have occurred by chance. If  $P > 0.05$ , the parameter is considered insignificant; if  $P < 0.05$ , the parameter is considered significant.

The results displayed in the analysis of variance table indicate that the two models are significant since the probability of significance of the risk p-value is less than 0.05, so we can say that the two models are well adjusted. Therefore, both models can be used to navigate the entire space of the experimental domain.

The ANOVA analysis of variance for the horizontal displacement  $U_x$  are presented in Table 4. The functional relationship between the output variables (horizontal displacement and safety factor) and the input variables ( $L$ ,  $Sv$ ,  $EA$ ) was expressed with a coefficient of determination ( $R^2= 99.63\%$  for  $U_x$  and  $R^2= 99.95\%$  for  $F_s$ ) which is the ratio between the variation due to the model and the total variation, shows that the model has a good adjustment for the two answers. The table also indicates the value of the residual standard deviation, the value of the average of the responses and the number of tests carried out.

On the other hand, the analysis of variance ANOVA presented in Table 6, shows that the normal stiffness of the geogrids ( $EA$ ) and the length of the geogrids, are the most important factors in the recess of the wall reinforced by geogrids, their contributions are 16.58%, for the geogrid normal stiffness ( $EA$ ) is 96.61% for the length of the geogrids, then the geogrid spacing ( $Sv$ ) with a percentage contribution of 11.84%. Therefore, the regression is highly significant and the model for each response is deemed to be consistent.

For interaction terms ( $L*EA$ ,  $Sv*EA$ ) have small contributions and the quadratic term ( $EA^2$ ) has no significant effect on the result.

**Abbreviations used in the results tables of ANOVA:**

SS: Sum Squares ;  
 MS: Mean of Squares ;  
 C% : % of Contribution.  
 S: Significant;  
 NS: Non Significant;  
 R : Remark

**Table 6 ANOVA statistical results of the response surface quadratic model horizontal displacement  $U_x$**

Source	SS	df	MS	F-value	P-value	C	R
Mode 1	4.14	9	0.4598	752.42	< 0.0001	99.75	S
A-L	0.1008	1	0.1008	164.98	< 0.0001	2.42	S
B-SV	0.4916	1	0.4916	804.44	< 0.0001	11.84	S
C-EA	0.6884	1	0.6884	1126.55	< 0.0001	16.58	S
AB	0.3039	1	0.3039	497.40	< 0.0001	7.32	S
AC	0.4796	1	0.4796	784.93	< 0.0001	11.55	S
BC	0.0289	1	0.0289	47.31	< 0.0001	0.69	S
$A^2$	2.16	1	2.1600	3528.07	< 0.0001	0.52	S
$B^2$	0.0603	1	0.0603	98.73	< 0.0001	1.45	S
$C^2$	0.0169	1	0.0169	27.63	< 0.0001	0.40	S
residual	0.0098	16	0.0006			0.23	
Total	4.15	25					

**Table 7 ANOVA statistical results of the response surface quadratic model safety factor  $F_x$**

Source	SS	df	MS	F-value	P-value	%C	R
Model	2.95	9	0.3277	3646.43	< 0.0001	100	S
A-L	2.85	1	2.85	31712.96	< 0.0001	96.61	S
B-Sv	0.0156	1	0.0156	173.66	< 0.0001	0.5288	S
C-EA	$8.23 \times 10^{-6}$	1	$8.23 \times 10^{-8}$	0.0009	0.9762	$2.78 \times 10^{-4}$	NS
AB	0.004	1	0.004	44.88	< 0.0001	0.135	S
AC	$9.39 \times 10^{-6}$	1	$9.39 \times 10^{-6}$	0.1047	0.7507	$3.18 \times 10^{-4}$	NS
BC	0.0001	1	0.0001	0.8340	0.3745	$3.389 \times 10^{-3}$	NS
$A^2$	0.0313	1	0.0313	348.55	< 0.0001	10.61	S
$B^2$	0.0004	1	0.0004	4.31	0.0544	0.0135	S
$C^2$	$2.89 \times 10^{-8}$	1	$2.89 \times 10^{-8}$	0.0003	0.9859	$9.79 \times 10^{-7}$	NS
Residual	0.0014	16	0.0001			0.058	
Total	2.95	25				100	

## 6.1 Regression Model Development

All of the essential adjustment characteristics of the postulated model are grouped in Tables 7 and 8. the responses surfaces provides a reasonably accurate estimate of slope failure probability and has a high computational efficiency (Dian-qiang, 2016).

The calculation of the coefficients of the factors and their interaction as well as the evaluation of their significant aspect allowed us to predict the polynomial models which are presented by the corresponding Equations 2 and 3.

$$U_x = -2.49128 + 0.889466 * L + 0.596673 * Sv + 0.000453 * EA + 0.106100 * L * Sv - 0.000071 * L * EA - 0.000098 * Sv * EA - 0.067535 * L^2 - 0.423095 * Sv^2 + 5.37869 * EA^2 \quad (2)$$

$$F_x = 2.13 + 0.4144 * L - 0.0294 * Sv - 0.0001 * EA + 0.0183 * L * Sv + 0.0009 * L * EA + 0.0025 * Sv * EA - 0.0733 * L^2 - 0.0085 * Sv^2 + 0.0001 * EA^2 \quad (3)$$

The functional relationship between the output variables (horizontal displacement and safety factor) and the input variables (L, Sv, EA) was expressed with a determination coefficient ( $R^2 = 99.63\%$  for  $U_x$  and  $R^2 = 99.95\%$  for  $F_x$ ) which is the ratio between the variation due to the model and the total variation, shows that the model has a good fit for both responses to verify that a model is adequate, the  $R^2$  value cannot be low than 0.75 (Le Man, 2010) (Benzannache, 2021). As a result, the model achieved good predictive adequacy. In a accordance with (Rai, 2016) satisfactory agreement requires a difference of less than 20% between Adj  $R^2$  and Pred  $R^2$ . Since Predicted  $R^2$  is 0.9765, the current study satisfies this criteria (Belaadi, 2023).

The analysis of the results shows that the predicted values and the numerical values are very close and in good agreement, this indicates the high precision of the model found.

According to Figures 14 and 15, the residuals of the model of the horizontal displacement and of the factor of safety can be judged as normally distributed. It was necessary for residuals to vary uniformly, so the residual point were symmetrically distributed with clustering close to the plot's center (Belaadi, 2023).

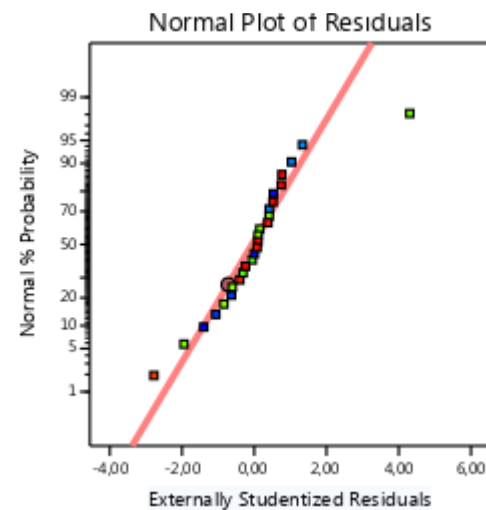


**Figure 14 Normal probabilities of safety factor residuals  $F_x$**

The response surface graphs in Figures 16 and 17 represent the results of the response surface (3D) of the horizontal displacement  $U_x$ , and the safety factor  $F_x$  as a function of the input parameters (L, Sv, B). The analysis of the response surfaces confirms the results of the ANOVA, we notice that the normal stiffness (EA) of the geogrids is important and has the great influence on the horizontal displacement, while the length of the reinforcement (L) has the most significant effect on the safety factor  $F_x$ .

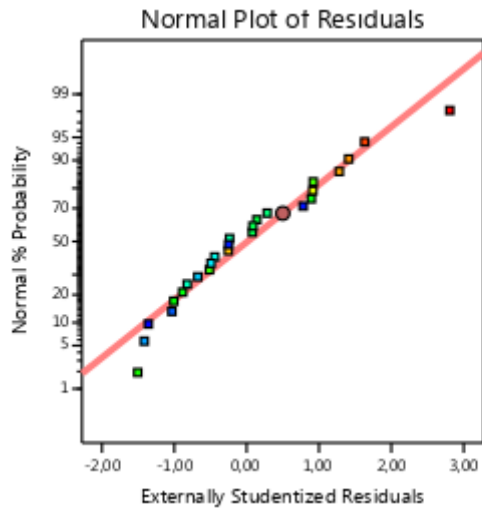


**Figure 15** Normal probabilities of the residues of the horizontal displacement  $U_x$

## 6.2 Graphical Representation of Response Surfaces

The contour graphs make it possible to visualize the response surface, and also to limit the ranges of variation of the response values and the desirable operating conditions, thus the response surfaces can present the variations of the responses according to only 2 factors to time, with the other factors set to a fixed value. Figures 16 and 17 show the response surfaces associated with geogrid-reinforced wall models.

Figures 16 and 17 show the 3D responses surfaces for the evolution of the safety factors and horizontal displacement corresponding to the interaction effects of the input parameters ( $L, Sv$  and EA) in the designed space, based on the regression equations listed above.

These observations may be applied to the two responses which confirmed the results of the ANOVA analysis.

The contour graphs make it possible to visualize the response surface, and also to limit the ranges of variation of the response values and the desirable operating conditions, thus the response surfaces can present the variations of the responses according to only 2 factors to that time. From which it is clearly noticed that the horizontal displacement response is strongly influenced by the normal stiffness (EA) of the geogrids, while the length of the reinforcement ( $L$ ) has the most significant effect on the safety factor Fs.

## 6.3 Optimization of the Parameters $L$ , $Sv$ , and EA.

An optimization process is conducted to determine the appropriate input parameter values required to achieve the desired process outcome. Typical optimization goals encompass maximizing process yield, minimizing the processing time needed for product manufacturing, or meeting a specified target product requirement. In this study, the optimization involves three key input variables:  $L$ ,  $Sv$ , and EA. The length of the reinforcement ( $L$ ) varies within the range of 3m to 9m, while the normal stiffness (EA) of the geogrid layers ranges between 2000 KN/m and 4000 KN/m, and the geogrid spacing  $Sv$  varies between 1m and 2m.

The constraints employed during the optimization process are outlined in Table 8. The core of the challenge is to focus on the desirability function ( $D$ ), which serves as the objective function while accounting for variable limitations. Table 9 visually presents the optimal parameter values for the examined problem.

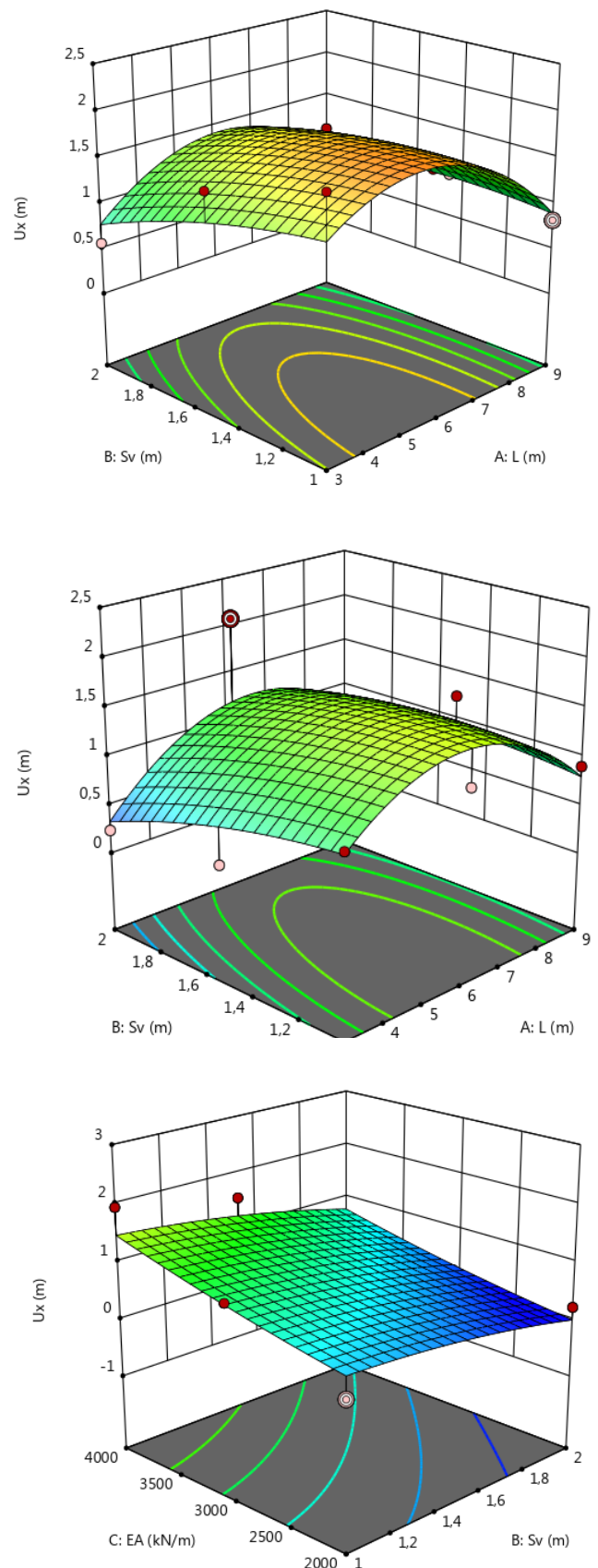


**Figure 16** Responses surfaces for the error function as a function of  $(L, Sv, EA)$  for  $U_x$

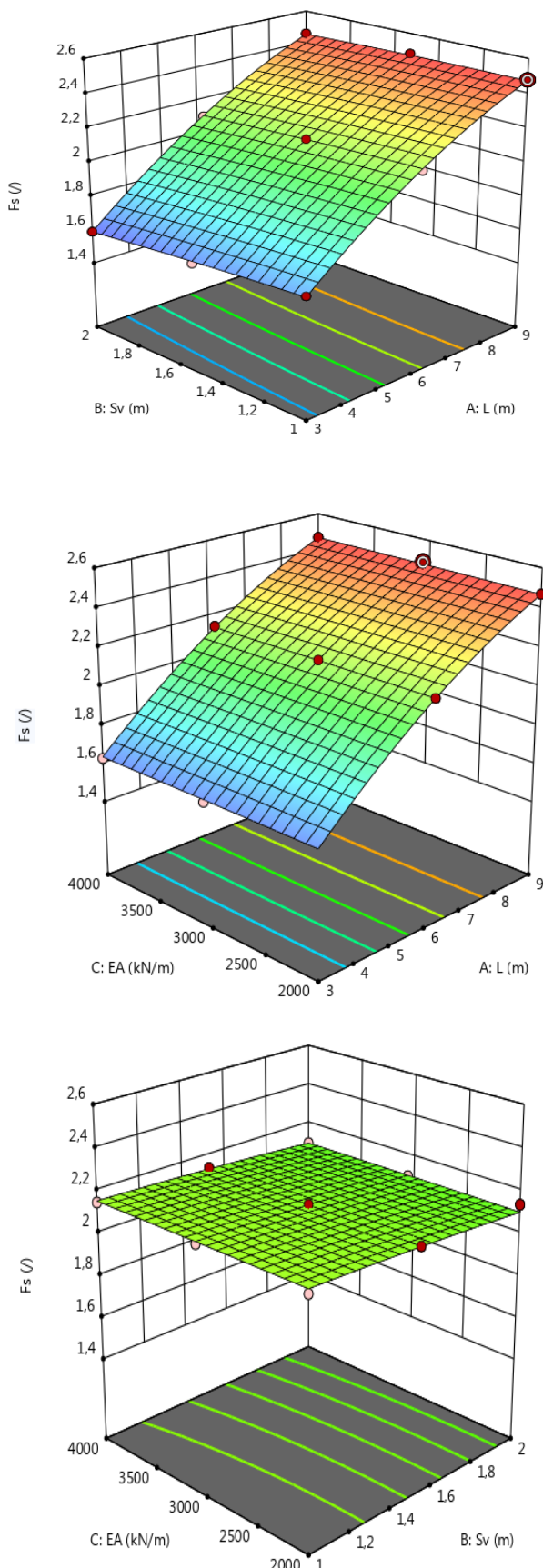


Figure 17 Responses surfaces for the error function as a function of (L,Sv,EA) for Fs

Table 8 Constraints applied to the parameters to be optimized

Parameters	Objective	Lower limit	Upper Limit
L (m)	In the rang	3	9
Sv (m)	In the rang	1	2
EA(kN/m)	In the rang	2000	4000
Ux (m)	Maximisation	0.0018	1.81
Fs	Minimization	1.58	2.48

#### 6.4 Model Validation by Experiments

The validity and predictability of models developed at numerical optimization were verified by experimental runs, in our model the experimental tests are replaced by a digital modeling by 2D plaxis as an attempt (Benchekikh, 2020). To validate the predicted results from the model, triplicate experiment runs were conducted under the optimal conditions. The comparison between the modeling and predicted values, as presented in Table 9, revealed no significant difference. This finding confirms the predictability of the model developed using RSM based on the central composite design CCD. Consequently, the proposed model in this study can be deemed reliable and applicable for reuse within the designated ranges of the design.

Table 9 Optimization results

Parameters	Values Optimized	Responses			
		Num	Pred	Num	Pred
Sv (m)	1				
L (m)	6	2.12	1.805	1.654	2.146
EA (kN/m)	4000				

#### 7. CONCLUSIONS

The work presented and divided into two parts, the first part helped to provide a good understanding of the problem of modeling retaining walls reinforced by geogrids and study the influence of geogrid length, vertical spacing between geogrid sheets, overload, mechanical properties of the reinforced soil, normal geogrid stiffness on the performance of reinforced soil retaining walls. The second part is an attempt to optimize the parameters influencing the stability of a synthetic retaining wall, namely the vertical spacing between the geogrids (Sv), the length (L) and the normal stiffness (EA), by the use of the response surface method via digital experimental plans through a composite L26 central type fractional plan, from digital calculation by the finite element software Plaxis 2D. This statistical method makes it possible to model the relationship between the input variables (L, Sv and EA), to predict the performance of synthetic retaining structures and to optimize their design. The importance of this parametric study is revealed with the highlighting of the major interest of the geogrid length, The number of horizontal reinforcing, the axial stiffness (EA) and the choice of backfill soil in the reduction of the horizontal displacements of the wall as well as the safety coefficient increases. Moreover this study aims to estimate the effect of the factors (L, Sv and EA) and the interactions of these parameters on the responses (Ux and Fs) in order to identify among them the statistically influential elements of the behavior of the wall reinforced by geogrids, including it is clearly noticed that the horizontal displacement response is strongly influenced by the normal stiffness (EA) of the geogrids, while the length of the reinforcement (L) has the most significant effect on the safety factor Fs.

## 8. LIST OF NOTATION AND ABBREVIATIONS

L :	Length of the geogrids,
CCD:	Central composite design ,
RSM:	Response surface methodology,
Sv:	Vertical spacing between reinforcements,
EA:	Normal stiffness,
SS:	Sum Squares,
MS:	Mean of Squares,
Ux :	Horizontal displacement,
Fs:	Safety factor,
C :	Cohesion,
φ :	Angle of friction,
ANOVA:	Analysis of variance,

## 9. ACKNOWLEDGMENTS

I should like to express my thanks to all those who have contributed to the achievement of these conclusive results, mostly Laboratory of Civil Engineering and Hydraulics, University 8 May 1945 Guelma, Algeria and Mr. Belabed Lazhar.

## 10. REFERENCES

Abd. A. H., Utili. S. (2017a). "Design of Geosynthetic-Reinforced Slopes in Cohesive Backfills. Geotext." *Geomembranes*. 45, 627 – 641, <https://doi.org/10.1016/j.geotexmem.2017.08.004>.

Abd. A. H., Utili. S. (2017b). "Geosynthetic-Reinforced Slopes in Cohesive Soils Subject to Seismic Action." *Procedia Eng.* 189, 898 – 907, <https://doi.org/10.1016/j.proeng.2017.05.140>.

Abdulhameed, A. S., Firdaus Hum, N. N. M., Rangabhashiyam, S., Jawad, A. H., Wilson, L. D., Yaseen, Z. M., Al-Kahtani, A. A., and Alothman, Z. A. (2021). " Statistical Modeling and Mechanistic Pathway for Methylene Blue Dye Removal by High Surface Area and Mesoporous Grass-based Activated Carbon using K<sub>2</sub>CO<sub>3</sub> Activator." *J. Environ. Chem. Eng.* 9, 105530, doi. org/10.1016/J.JECE.2021.105530.

Adamu, M., Trabanpruek, P., Jongvivatsakul, P., Likitlersuang, S. et Iwanami, M. (2021). "Mechanical Performance and Optimization of High-Volume Fly Ash Concrete Containing Plastic Wastes and Graphene Nanoplatelets using Response Surface Methodology." *Construction and Building Materials*, Vol. 308, 125085, <https://doi.org/10.1016/j.conbuildmat.2021.125085>.

Adamu, M., Trabanpruek, P., Limwibul, V., Jongvivatsakul, P., Iwanami, M. et al., Likitlersuang, S. (2022). "Compressive Behavior and Durability Performance of High-Volume Fly-Ash Concrete with Plastic Waste and Graphene Nanoplatelets by using Response-Surface Methodology." *Journal of Materials in Civil Engineering* Vol. 34, No. 9, Article no. 04022222, doi.:10.1061/(ASCE)MT.1943-5533.0004377.

Amidou, S., (1995). "Ouvrages Renforcés Par Géotextiles Chargés en Tête : Comportement et Dimensionnement, Thèse de Doctorat Présentée à L'Ecole Nationale Des Ponts Et Chaussees, <https://pastel.hal.science/tel-00529482>.

Bathurst, R. J., Nernheim, A., Walters, D. L., Allen, T. M., Burgess, P. and Saunders, D. D. (2009). "Influence of Reinforcement Stiffness and Compaction on the Performance of Four Geosynthetic-Reinforced Soil Walls." *Geosynthetics International*, 16, No. 1, 43–59, doi: 10.1680/gein.2009.16.1.43.

Barret, J. R., (1966). "Use of Plastic Filters in Costal Structures." *Proceedings of 10th Int. Conf. on Coastal Engineering*, Tokyo, 1048-1067.

Beckham, W. K., Mills, W. H. (1935). "Cotton-Fabric-Reinforced Roads." *Engineering News Record*, Vol. 115, no. 14, 453- 455.

Belaadi, A., Abdelaziz Lekrine, A., Boumaaza, M. et al. (2023). "Water Uptake of HDPE Reinforced with Washingtonia Fiber Biocomposites: Mathematical Modeling using Artificial Neural Network, Response Surface Methodology and Genetic Algorithm." *Advances in Materials and Processing Technologies*, DOI: 10.1080/2374068X.2023.2198828.

Benzannache, N., Belaadi, A., M. Boumaaza, M., Bourchak, M. (2021). "Improving the Mechanical Performance of Biocomposite Plaster/Washingtonian Filifirafibres using the RSM Method." *Journal of Building Engineering*. 33:33, doi:10.1016/j.jobe.2020.101840.

Bian, J., Gu, Y., and Murray, M. H. (2013). "A Dynamic Wheel-Rail Impact Analysis of Railway Track Under Wheel Flat by Finite Element Analysis." *International Journal of Vehicle System Dynamics*, Taylor & Francis Group, 51(6), 784-797, <https://doi.org/10.1080/00423114.2013.774031>.

Bingquan, H., Richard, J., Bathurst, H., and Kianoosh, H. (2009). "Numerical Study of Reinforced Soil Segmental Walls Using Three Different Constitutive Soil Models." *Journal of Geotechnical and Geoenvironmental Engineering*, DOI: 10.1061/(ASCE)GT.1943-5606.0000092.

Boumezerane, D. (2022). "Recent Tendencies in the Use of Optimization Techniques in Geotechnics: A Review." *Geotechnics*. 2, 114–132, <https://doi.org/10.3390/geotechnics2010005>.

Boutahir Born Bencheikh., M. Aidoud, A., Benamara, F. Z., Belabed, L., and Dorbani, M. (2021). "An Attempt to Apply the Kinematic Method of Rigid Solids in the Study of Bearing Capacity of Shallow Foundations." *Selected Scientific Papers - Journal of Civil Engineering*. Vol. 16, 175-187, <https://doi.org/10.18280/acsm.450603>.

Boutahir Born Bencheikh., M. Aidoud, A., Benamara, F. Z., (2020). "Contribution to the Study of Soil Stabilized by Ballast Columns." *Civil and Environmental Engineering Reports*. Vol. 30 3, 234-252, DOI: 10.2478/ceer-2020-0042.

Carroll, R. G., Walls, J.C., Haas, R. (1987). "Granular Base Reinforcement of Flexible Pavements using Geogrids." *Proceedings, Vol. 1, Geosynthetics '87 Conference, New Orleans, USA*, 46-57.

Chao, K. C., Overton, D. D., and Nelson, J. D. (2006). "Design and Installation of Deep Benchmarks in Expansive Soil." *Journal of Surveying Engineering*, American Society of Civil Engineers, 132(3), 124-131, DOI:10.1061/(ASCE)0733-9453.

Dian-qing, L., Dong, Z., Zi-jun, C., Xiao-song, T., Kokkwang, P. (2016). "Response Surface Methods for Slope Reliability Analysis." *Review and comparison. Journal of Engineering Geology*. Vol. 203, 3–14, <https://doi.org/10.1016/j.enggeo.2015.09.003>.

Ebba, M., Asaithambi, P., Alemayehu, E. (2022). "Development of Electrocoagulation Process for Wastewater Treatment: Optimization by Response Surface Methodology." *Heliyon* 8, e09383, <https://doi.org/10.1016/J.HELIYON.2022.E09383>.

Fragaszy, R. J., Lawton, E. (1984). "Bearing Capacity of Reinforced Sand Subgrades." *Journal of Geotechnical Engineering Division*, 110 (10), 1500-1507, [https://doi.org/10.1061/\(ASCE\)0733-9410\(1984\)110:10\(1500\)](https://doi.org/10.1061/(ASCE)0733-9410(1984)110:10(1500)).

Gaudio, D., Masini, L., Rampello, S. (2018). "Seismic Performance of Geosynthetic-Reinforced Earth Retaining Walls Subjected to Strong Ground Motions." *Proceedings of China-Europe Conference on Geotechnical Engineering, SSGG*. Springer International Publishing, 1474–1478, <https://doi.org/10.1007/978-3-319-97115-5>.

Ghelich, R., Jahannama, M. R., Abdizadeh, H., Torknik, F. S., Vaezi, M. R. (2019). "Central Composite Design (CCD)-Response Surface Methodology (RSM) of Effective Electrospinning Parameters on PVP-B-Hf Hybrid Nanofibrous Composites for Synthesis of HfB<sub>2</sub>-Based Composite Nanofibers." *B Eng.* 166 (2019) 527–541, DOI:10.1016/j.compositesb.2019.01.094.

Gicot, O., Perfetti, J. (1982). "Géotextiles : Conceiving and Design Engineering structures." *Rhône-Poulenc Fibres, Bezons, France*, 256.

Giroud, J. P., Noiray, L. (1981). "Geotextile Reinforced Unpaved Road Design." *Journal of the Geotechnical Engineering Division*, 107, 1233-1254, <https://doi.org/10.1061/AJGEB6.0001187>.

Hamderi, M., Guler, E., Demirkhan, M., (2007). "Numerical Analysis of Reinforced Soil Retaining Wall Structures with Cohesive and Granular Backfills." *Geosynthetics International*, 14, No. 6, 330-345, DOI:10.1680/gein.2007.14.6.330.

Hardiyatmo, H. C. (1995). "Experimental Approach to the Dimensioning of Reinforced Blocks with Cellular Facing." *Doctoral Thesis; Doctoral Thesis*, Université Joseph Fourier Grenoble, France.

Hicham Alhajj, C. (2016). "Geosynthetic-Reinforced Retaining Walls, Deterministic and Probabilistic Approaches." *Doctoral Thesis*, University Grenoble Alpes.

Huang, X., Lv, Z., Zhao, B., Zhang, H., Yao, X., Shuai, Y. (2022). "Optimization of Operating Parameters for Methane Steam Reforming Thermochemical Process using Response Surface Methodology." *Int. J. Hydrogen Energy*, 47, 28313–28321, <https://doi.org/10.1016/I.IJHYDENE.2022.06.166>. Latha, G.M.

Huang, B., Bathurst, R. J., Hatami, K., Allen, T. M. (2010). "Influence of Toe Restraint on Reinforced Soil Segmental Walls." *Canadian Geotechnical Journal*, 47(8), 885-904, 2010, <https://doi.org/10.1139/T10-002>.

Humphreys, M. P., Armstrong, L. W. (1993). "Assessing the Sensitivity of Numerical Models using Response Surface Methodology." *Proceedings of the Conference of Probabilistic Methods in Geotechnical Engineering, Canberra, Australia*, 135–144, DOI. <https://doi.org/10.1201/9781003077749>.

Jirawattanasomkul, T., Kongwang, N., Jongvivatsakul, P. et Likitlersuang, S. (2019). "Finite Element Analysis of Tensile and Puncture Behaviours of Geosynthetic Cementitious Composite Mat (GCCM)" *Composites Part B: Engineering*, Vol. 165, 15 May, 702-711, <https://doi.org/10.1016/j.compositesb>.

Jirawattanasomkul, T., Kongwang, N., Jongvivatsakul, P. et Likitlersuang, S. (2018). "Finite Element Modelling of Flexural Behaviour of Geosynthetic Cementitious Composite Mat (GCCM)." *Composites Part B: Engineering*, Vol. 154, 33-42, <https://doi.org/10.1016/j.compositesb.2018.07.052>.

Jongvivatsakul, P., Ramdit, T., Ngo, T. P. et al., Likitlersuang, S. (2018). "Experimental Investigation on Mechanical Properties of Geosynthetic Cementitious Composite Mat (GCCM)." *Construction and Building Materials*, Vol. 166, 30, 956-965, <https://doi.org/10.1016/j.conbuildmat.2018.01.185>.

Lakehal, R., Djemili, L., Houichi, L. (2011). "Nomograms for Calculating the Safety Factor of Homogeneous Earth Dams in Long-Term Stability." *African Journal of Environmental Science and Technology*, Vol. 5, No. 9, 755–759, <http://www.academicjournals.org/AJEST>.

Lakehal, R., Djemili, L. (2017). "Studying the Effect of a Variation in the Main Parameters on Stability of Homogeneous Earth Dams using Design Experiment." *Journal of Water and Land Development*, No. 34, 173–179, DOI: 10.1515/jwld-2017-0051.

Laxmikant, Y., Tripathi, R.K. (2013). "Effect of the Length of Geogrid Layers in the Bearing Capacity Ratio of Geogrid Reinforced Granular Fill-soft Subgrade Soil System." *Procedia - Social and Behavioral Sciences*, Vol. 104, 2 December 2013, 225-234, <https://doi.org/10.1016/j.sbspro.2013.11.115>.

Le Man, H., Behera, S. K., Park, H. S. (2010). "Optimization of Operational Parameters for Ethanol Production from Korean Food Waste Leachate." *International Journal of Environmental Science & Technology*, 7, 157–164, <https://doi.org/10.1007/BF03326127>.

Leshchinsky, D., Han, J. (2004). "Geosynthetic Reinforced Multitiered Walls." *J. Geotech. Geoenvironmental Eng.* 130, 1225–1235, [https://doi.org/10.1061/\(ASCE\)10900241130:12\(1225\)](https://doi.org/10.1061/(ASCE)10900241130:12(1225)).

Leshchinsky, D., Vulova, C. (2001). "Numerical Investigation of the Effects of Géosynthétique Spacing of Failure Mechanism." *MSE blok wall, Geosynthetics International*, 8(4):343-365, DOI:10.1680/gein.8.0199.

Love, J. P., Burd, H. J., Milligan, G. W. E., Houlsby, G. T. (1987). "Analytical and Model Studies of Reinforcement of a Layer of Granular Fill on a Soft Clay Subgrade." *Canadian Geotechnical Journal*, 24, 611-622, <https://doi.org/10.1139/t87-075>.

Mahmoud, M. A., Abdrabbo, F. M. (1989). "Bearing Capacity Tests on Strip Footing on Reinforced Sand Subgrade." *Canadian Geotechnical Journal*, 26, 154-159, DOI: 10.1139/t89-015.

Mandal, J. M., Manjunath, V. R. (1995). "Bearing Capacity of Strip Footing Resting on Reinforced Sand Subgrades." *Construction and Building Material*, 9 (1), 35-38, [https://doi.org/10.1016/0950-0618\(95\)92858-E](https://doi.org/10.1016/0950-0618(95)92858-E).

Masini, L., Callisto, L., Rampello, S. (2015). "An Interpretation of the Seismic Behaviour of Reinforced-Earth Retaining Structures." *Géotechnique*, 65, 349–358, <https://doi.org/10.1680/g-eot.sip.15.p.001>.

Ngo, T. P., Likitlersuang, S., Takahashi, A. (2019). "Performance of a Geosynthetic Cementitious Composite Mat for Stabilising Sandy Slopes." *Geosynthetics International*, Vol. 26, issue 3, 309-319, <https://doi.org/10.1680/jgein.19.00020>.

Ngo, T. P., Takahashi, A. et al., Likitlersuang, S. (2023). "Centrifuge Modelling of a Soil Slope Reinforced by Geosynthetic Cementitious Composite Mats." *Geotechnical and Geological Engineering*, 41(1), DOI: 10.1007/s10706-022-02311-6.

Rai, A., Mohanty, B., Bhargava, R. (2016). "Supercritical Extraction of Sunflower Oil: A Central Composite Design for Extraction Variables." *Food Chemistry*, 192, 647–659, <https://doi.org/10.1016/j.foodchem.2015.07.070>.

Salari, M., Nikoo, M. R., Al-Mamun, A., Rakhshandehroo, G. R., Mooselu, M. G. (2022). "Optimizing Fenton-like Process, Homogeneous at Neutral pH for Ciprofloxacin Degradation: Comparing RSM-CCD and ANN-GA." *J. Environ. Manag.* 317 (2022), 115469, <https://doi.org/10.1016/J.JENVMAN.2022.115469>.

Santhanakumar, P. (2015). "Seismic Response of Reduced-Scale Modular Block and Rigid Faced Reinforced Walls through Shaking Table Tests. Geotext." *Geomembranes*, 43, 307–316, <https://doi.org/10.1016/j.geotexmem.2015.04.008>.

Sivakumar Babu, G. L., Srivastava, A. (2007). "Reliability Analysis of Allowable Pressure on Shallow Foundation using Response Surface Method." *Computers and Geotechnics*, Vol. 34, issue 3, 187–194, DOI: 10.1016/j.compgeo.2006.11.002.

Somayajula, A., Asaithambi, P., Susree, M., Matheswaran, M. (2012). "Sonochemical Oxidation for Decolorization of Reactive Red 195." *Ultrason. Sonochem*, 19, 803–811, <https://doi.org/10.1016/J.ULTSONCH.2011.12.019>.

Sukkarak, R., Jongpradist, P., Kongkitkul, W., Jamsawang, P., Likitlersuang, S. (2021). "Investigation on Load-Carrying Capacity of Geogrid-Encased Deep Cement Mixing Piles." *Geosynthetics International*, Vol. 28, issue 5, 450-463, <https://doi.org/10.1680/jgein.21.00026>.

Surarak, C., Likitlersuang, S., Wanatowski, D., Balasubramaniam, A., Oh, E. et Guan, H. (2012). "Stiffness and Strength Parameters for Hardening Soil Model of Soft and Stiff Bangkok Clays." *Soils and Foundations*, Vol. 52, no. 4, 682–697, doi:10.1016/j.sandf.2012.07.009.

Tandjiria, V., The, C. I., Low, B. K. (2000). "Reliability Analysis of Laterally Loaded Piles using Response Surface Methods." *Structural Safety*, Vol. 22, 335–355, [https://doi.org/10.1061/\(ASCE\)1090-0241](https://doi.org/10.1061/(ASCE)1090-0241).

Verma, B. P., Char, A. N. R. (1986). "Bearing Capacity Tests on Reinforced Sand Subgrades." *Journal of Geotechnical Engineering*, 112 (7), 701-706, [https://doi.org/10.1061/\(ASCE\)0733-9410](https://doi.org/10.1061/(ASCE)0733-9410).

Wilson-Jones, H. (1992). "Structures Reinforced with Geosynthetics in a Flat Analog Model." *Doctoral Thesis, Geotechnics, Joseph-Fourier University –Grenoble*.

I. French., Wong., F. S. (1985). "Slope Reliability and Response Surface Method." *Journal of Geotechnical and Geoenvironmental Engineering*, Vol. 111, 32–53, [https://doi.org/10.1061/\(ASCE\)0733-9410.13.3.9410](https://doi.org/10.1061/(ASCE)0733-9410.13.3.9410).